Improving buried object localization accuracy in heterogeneous environments using TOA-based IR-UWB and machine learning

Nguyen Thi Huyen[1], Duong Duc Ha[1*], Giap Viet Anh[1], Luu Dinh Nam[1], Tran Thi Hoa[2]

[1]Faculty of Radio and Electronics Engineering, Le Quy Don Technical University, 236 Hoang Quoc Viet, Nghia Do, Hanoi, Vietnam;
[2]Thai Binh University, 142-144 Le Loi, Thai Binh, Hung Yen, Vietnam.
[*]Corresponding author: duongha@lqdtu.edu.vn

Received 06 May 2026; Revised 26 Jun. 2026; Accepted 29 Jun. 2026; Published 25 Aug. 2026.
DOI: https://doi.org/10.54939/1859-1043.j.mst.113.2026.3-11

ABSTRACT

This paper proposes a buried-object localization method in heterogeneous environments using time of arrival (TOA)-based Impulse Radio UWB (IR-UWB) radar and machine learning techniques. A propagation model is developed to generate a TOA dataset for buried-object locations under multipath and noisy conditions. To improve TOA estimation, a matched-filtering and adaptive-thresholding (MFAT) technique is proposed to enhance reflected pulse detection at low SNR. The extracted TOA features are then used to train Random Forest (RF), XGBoost, and LightGBM (LGBM) models for object localization. Experimental results show that the proposed LGBM-MFAT approach achieves the best performance, with an MAE of 1.26 cm, an RMSE of 2.37 cm, and an R^2 *value of 0.999. The results demonstrate that combining adaptive TOA processing with gradient-boosting models significantly improves localization accuracy and provides an effective solution for penetrating IR-UWB radar systems operating in heterogeneous environments.*

Keywords: IR-UWB technology; Ground penetrating radar; TOA; Random Forest; XGBoost; LGBM.

1. INTRODUCTION

Ultra-Wideband (UWB) technology has attracted considerable attention for high-accuracy localization in complex and GNSS-denied environments due to its fine temporal resolution and strong resistance to multipath propagation [1-3]. Among UWB positioning techniques, TOA estimation remains the most widely used approach because of its clear physical interpretation and high ranging accuracy [4, 5]. In penetrating radar systems, however, TOA estimation is severely degraded by attenuation, clutter, and multipath propagation, particularly in heterogeneous environments [6-10]. Recent studies have demonstrated that machine learning and deep learning techniques can effectively model complex propagation characteristics and improve localization performance in UWB and GPR applications [11-15]. More recently, hybrid frameworks integrating physics-based signal processing with deep neural networks have emerged as an effective paradigm for RF localization and parameter estimation [16]. Nevertheless, accurate TOA extraction and reliable buried-object localization in multilayer media remain challenging because existing approaches generally process TOA estimation and localization separately while remaining sensitive to severe multipath and heterogeneous propagation.

To address these issues, this paper proposes a machine learning (ML)-based TOA processing framework for IR-UWB penetrating localization systems. Compared with Frequency-Modulated Continuous-Wave (FMCW) radar, IR-UWB offers superior penetration capability and range resolution due to its ultra-short pulses and direct TOF measurement [17]. The proposed architecture employs a matched-filtering and adaptive-thresholding (MFAT) technique for clutter suppression and background-noise mitigation to improve TOA estimation under low-SNR conditions. Subsequently, the extracted TOA features are processed using RF, XGBoost, and LightGBM models for accurate buried-object localization in heterogeneous environments.

The remainder of this paper is organized as follows. Section 2 describes the system model and methodology for the proposed approach. In Section 3, we present experimental results to evaluate the performance of the proposed method against previous techniques. Finally, Section 4 concludes the paper and outlines directions for future work.

2. PROBLEM

2.1. Proposed system model

A system using UWB technology for measuring the distance and positioning buried objects in heterogeneous environments is illustrated in Figure 1. The location of the buried object is defined in the 2-D space via the horizontal parameter of X_{ob} and the buried depth of Y_{ob}. The transmitted pulse $s(t)$ passes through the first layer, partly reflected at the boundary - at depth Y_0 from the ground, the rest is transmitted to the second layer, reflected at the buried object denoted by "O", and returned to the transceiver according to the direction $C \rightarrow B \rightarrow A$. The incidence and refraction angles when the device is at position X_{Dei} are denoted by φ_i and ψ_i, respectively.

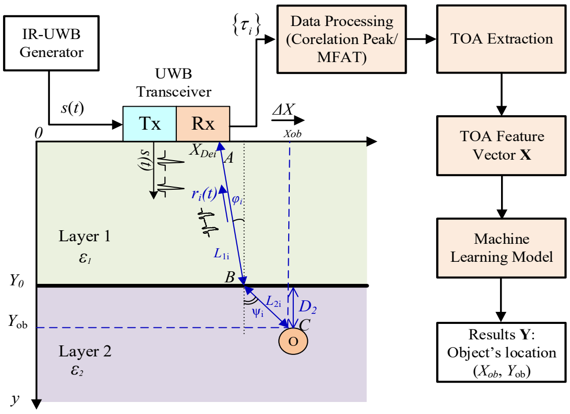

Figure 1. *Proposed model for locating the buried object in the heterogeneous environments.*

In an IR-UWB radar system, the transmitter emits a sequence of N impulse signals $s(t)$ at regular time intervals. The transmitted impulses can be mathematically expressed as follows:

$$s(t) = \sum_{n=0}^{N-1} g(t - nT_r), \tag{1}$$

where T_r is the repetition period of the pulse, $g(t)$ Gaussian pulse usually takes the form [18].

$$g(t) = A_p e^{-2\pi\left(\frac{t}{\mu_p}\right)^2}, \tag{2}$$

μ_p is the time normalization factor. The n^{th} derivative of a Gaussian pulse, named n^{th}-order monocycle, is:

$$g(t) = A_{np} \frac{d^n}{dt^n} e^{-2\pi\left(\frac{t}{\mu_p}\right)^2}. \tag{3}$$

Among the impulse waveforms commonly employed, the second-order monocycle pulse is the most widely used due to its pulse width and spectral characteristics.

In Figure1, the signals reflected from the boundary and the buried object at the i^{th} displacement of the device have the following forms:

$$r_{1i}(t) = A_1(L_{1i})A_{21}s(t-\tau_{0i}) + n_1(t), \tag{4}$$

$$r_{2i}(t) = A_2(L_{2i})(1-A_{21})s(t-\tau_{2i}) + n_2(t), \tag{5}$$

where A_1, A_2 are the attenuation factors relative to the distance of the environment with Layer 1 and Layer 2, respectively; A_{21} is the reflection factor from the boundary between two layers; $n(t)$ is AWGN, τ_{0i}, τ_{2i} are TOAs of received pulses. At the i^{th} displacement of the transceiver, $\{L_{1i}\}$ $\{L_{2i}\}$ which are the propagation distances from the device to the boundary, and from the boundary to the buried object, respectively, could be determined based on the TOA as follows.

$$L_{1i} = \frac{1}{2}V_1\tau_{0i} = \frac{1}{2}\frac{c}{\sqrt{\varepsilon_1}}\tau_{0i}, L_{2i} = \frac{1}{2}V_2(\tau_{2i}-\tau_{0i}) = \frac{1}{2}\frac{c}{\sqrt{\varepsilon_2}}(\tau_{2i}-\tau_{0i}), \tag{6}$$

where V_i is the wave velocity in the i^{th} layer of the environment and c is the speed of light in vacuum. The TOA parameters are determined by the peak of the cross-correlation function.

$$R(\tau) = \int r(t)s(t-\tau)dt\ ; \quad \tau_{TOA} = \text{Arg}\max_{\tau}\{R(\tau)\}. \tag{7}$$

Based on the measured TOA values, the coordinates of the buried object (X_{ob}, Y_{ob}) can be estimated using the relationships among the model parameters, expressed as follows.

$$\tau_{0i} = 2\frac{L_{1i}\sqrt{\varepsilon_1}}{c},\ \tau_{2i} = 2\left(\frac{L_{1i}}{V_1} + \frac{L_{2i}}{V_2}\right), Y_0 = \frac{1}{2}\min_i\{\tau_{0i}\}V_1, \tag{8}$$

$$\left(\frac{1}{2}(\tau_{2i}-\tau_{0i})V_2\right)^2 = (Y_{ob}-Y_0)^2 + \left(|X_{ob}-X_{Dei}| - \sqrt{\left(\frac{1}{2}\tau_{0i}V_1\right)^2 - Y_0^2}\right)^2. \tag{9}$$

Although the Levenberg–Marquardt algorithm [19] can be used for buried-object localization, its high computational complexity and sensitivity to convergence motivate the use of machine learning models.

2.2. Data preprocessing and machine learning method

2.2.1. Data preprocessing

The TOA dataset was generated using the GPR PRO tool for various buried-object locations in heterogeneous environments. Due to multipath propagation, the received signals contain reflections from buried targets, layer interfaces, clutter, and background noise, making TOA estimation challenging. To address this issue, a Matched-Filtering and Adaptive-Thresholding (MFAT) technique is proposed to enhance the signal-to-noise ratio and improve echo detection. The matched filter employs the time-reversed transmitted pulse to generate distinct correlation peaks corresponding to the reflected echoes, which are subsequently processed by an adaptive leading-edge detector for accurate TOA estimation in multilayer propagation environments. The procedure is summarized as follows.

(i) The TOA detection threshold γ is determined based on the false alarm probability P_{FA} and the background noise power P_n:

$$\gamma = \alpha P_n; \quad P_n = \frac{1}{M}\sum_{k\in\kappa}|y(k)|^2; \tag{10}$$

M denotes the number of training cells, K represents the set of training cells used for estimating the noise and clutter power, and $y(k)$ denotes the output of the matched filter at the k-th time sample. In this study, the parameter is selected as M=32.

(ii) The scaling coefficient α is calculated according to the selected false alarm probability P_{FA}, with P_{FA}=0.01 adopted in this work:

$$\alpha = M\left(P_{FA}^{-1/M} - 1\right). \tag{11}$$

(iii) Accordingly, the TOA is estimated as follows:

$$\tau_{TOA} = \min\left\{t : \left|y(t)\right|^2 > \gamma\right\}; \tag{12}$$

2.2.2. Machine learning method

Tree-based machine learning models, including Random Forest (RF), XGBoost, and LightGBM (LGBM), have been widely employed in penetrating radar localization problems using TOA data. RF offers advantages such as implementation simplicity, high stability, and robustness against overfitting, making it an effective baseline model for regression tasks involving buried-object localization. However, its capability to capture highly complex nonlinear relationships is relatively limited in environments affected by background noise and multipath propagation. In contrast, XGBoost employs a gradient-boosting framework that enables efficient learning of nonlinear correlations between TOA measurements and target coordinates, providing strong performance in heterogeneous environments influenced by clutter, additive white Gaussian noise (AWGN), and multipath reflections. Similarly, LGBM represents an optimized boosting approach characterized by fast training speed and efficient processing of large-scale datasets. In this paper, RF, XGBoost, and LGBM are all implemented and evaluated to compare their localization performance under penetrating radar scenarios.

3. RESULTS AND DISCUSSION

3.1. Input data

The transmitted and received pulse signals were generated using the GPR PRO simulation tool with the 2nd order monocycle pulse at a center frequency of 4.0 GHz. The pulse time window was set to 5.12 ns, the relative permittivities varied within [3.5, 4.5], the interface depths were in [0.3, 0.4, 0.5] m, the radar scanned within [0, 3.0] m with a 10 cm step size, and the buried object positions varied within [0.01, 3.0] m in both horizontal and depth directions with an increment of 10 cm. The SNR was varied within [0, 20] dB resulting in a dataset comprising more than 85,000 samples corresponding to different buried-object locations in a heterogeneous medium. The dataset was split into training data (80%) and testing data (20%) for the machine learning models. To optimize the model and improve its generalization performance, 5-fold cross-validation was applied to the training set using the Scikit-learn library. A RandomizedSearchCV was conducted to identify the best hyperparameters based on evaluation metrics (MAE, MSE, RMSE) for each machine learning model and the results are shown in Table 1.

Table 1. *The hyperparameter sets of the machine learning models.*

Model	The hyperparameter
RF	n_estimators=300, max_depth=150, min_samples_split=10, max_samples=0.9, min_samples_leaf=4, max_features=5
XGBoost	n_estimators=300, learning_rate=0.01, max_depth=50, subsample=1.0, colsample_bytree=0.8
LGBM	n_estimators=300, learning_rate=0.01, max_depth=16, min_child_weight=2, colsample_bytree=0.8, feature_fraction=0.8, bagging_fraction=0.8

3.2. Evaluation metrics

The performance of the proposed method is evaluated using evaluation metrics such as Mean Absolute Error (MAE), Root Mean Squared Error (RMSE). The RMSE value of TOA estimation is compared with the Cramer-Rao lower bound (CRLB). Those parameters are calculated as follows:

$$MAE = \frac{1}{N}\sum_{i=1}^{N}\left|y_i - \hat{y}_i\right|, MSE = \frac{1}{N}\sum_{i=1}^{N}\left(y_i - \hat{y}_i\right)^2, RMSE = \sqrt{\sum_{i=1}^{N}\frac{\left(y_i - \hat{y}_i\right)^2}{N}}, \quad (13)$$

where N is the total number of samples; $\hat{y}_i$, y_i represent the estimated and observed TOA values, respectively. The CRLB on the standard deviation of an unbiased TOA estimator $\hat{\tau}$ is:

$$\sqrt{\mathrm{Var}\left(\hat{\tau}\right)} \geq \frac{1}{2\sqrt{2}\pi\sqrt{SNR}\Delta F}, \quad (14)$$

where SNR, ΔF are the signal to noise ratio and effective bandwidth, respectively.

Machine learning models were employed for two primary tasks: TOA estimation and buried-object localization. In the first task, the TOA values were determined using both the correlation-function peak method and the proposed MFAT approach. With the second task, for each buried-object location, the extracted TOA values obtained from N radar scanning positions are arranged into an input feature vector of the RF, XGBoost, and LightGBM models:

$$\mathbf{X} = \left[\tau_{i1}, \tau_{i2}, ..., \tau_{iN}\right] \in \mathbb{R}^{1\times N}, \; i = 1,2,...M, \quad (15)$$

where, M is the total number of data samples, N is the number of radar scan positions, τ_{ij} is TOA value of sample i at scan position j. The corresponding output vector is defined as:

$$\mathbf{Y} = \left[X_{ob,i}, Y_{ob,i}\right], \; i = 1,2,...M, \quad (16)$$

which $\left[X_{ob,i}, Y_{ob,i}\right]$ representing the horizontal coordinate and depth of the buried object, respectively. The machine learning models aim to learn a nonlinear mapping:

$$f : \mathbf{X} \to \mathbf{Y} \text{ or } \quad \hat{\mathbf{Y}} = f\left(\mathbf{X}\right). \quad (17)$$

The LightGBM model is trained by minimizing the mean squared error (MSE) loss function, defined as:

$$LF = \frac{1}{M}\sum_{i=1}^{M}\left[\left(X_{ob,i} - \hat{X}_{ob,i}\right)^2 + \left(Y_{ob,i} - \hat{Y}_{ob,i}\right)^2\right]. \quad (18)$$

3.3. Simulation results and comments

Firstly, we evaluate the effectiveness of applying the MFAT technique in data preprocessing. As observed from the results presented in Figure 2(a), the proposed MFAT technique significantly enhances the TOA estimation performance of all three machine learning models. Among all evaluated approaches, the LGBM-MFAT model demonstrates the best performance, achieving an RMSE of approximately 2.2 ns at SNR = 20 dB and around 20 ns at SNR = 0 dB. Overall, compared with the conventional TOA estimation method based on the correlation-function peak, the proposed MFAT technique reduces the estimation error by approximately 35–45%.

In comparison with the CRLB in Figure 2(b), a noticeable gap remains between the experimental results and the theoretical bound, particularly in low-SNR conditions. This discrepancy can be attributed to the severe effects of clutter, multipath propagation, and the heterogeneous characteristics of the transmission medium on the received signals in penetrating radar systems. Nevertheless, the integration of the MFAT technique substantially enhances the accuracy of TOA estimation, thereby improving localization performance in penetrating environments affected by noise and multipath propagation.

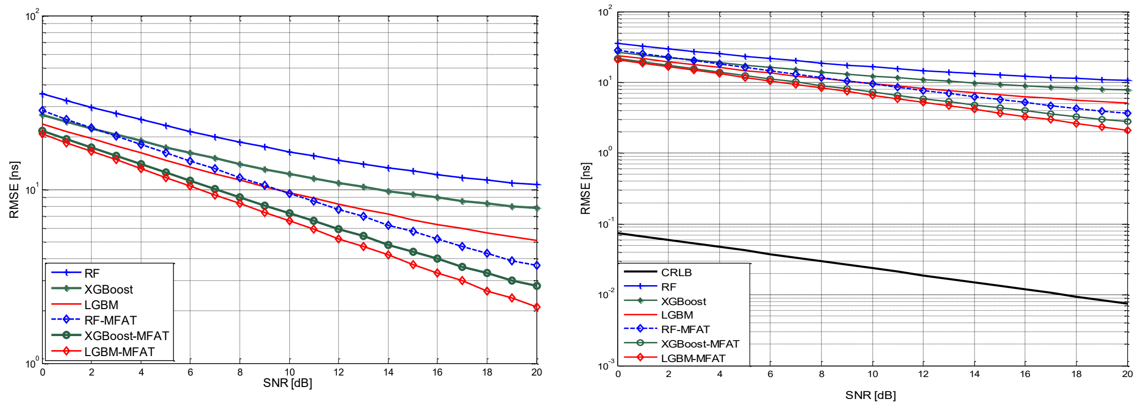

a) b)

Figure 2. *RMSE of TOA estimation obtained using different machine learning models (a), along with a comparison against the CRLB bounds (b)*

Secondly, the estimation results for the object's position in 2D space using the proposed method are presented as scatter plots for each coordinate component X_O and Y_O on the testing set shown in Figures 3 and Tables 2, 3. Figures 3 (a) and 3 (c) illustrate the scatter plots of the estimated coordinates of the buried object (X_O, Y_O) in the case without applying the MFAT technique for data preprocessing with LGBM model, while the results obtained using the MFAT technique with LGBM model are shown in Figures 3 (b) and 3 (d), respectively. The values of the evaluation metrics are illustrated in Table 2 and the comparison between the proposed method and other approaches using the MAE, RMSE indicators is shown in Table 2.

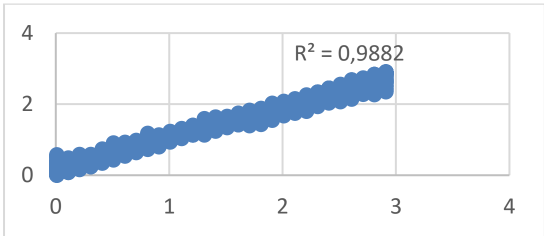

a) Scatter plot of X_O estimates without MFAT

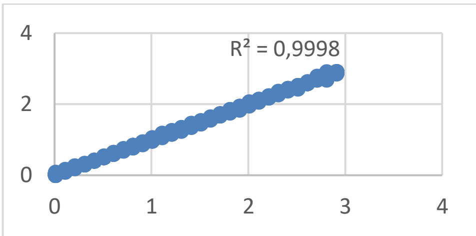

b) Scatter plot of X_O estimates with MFAT

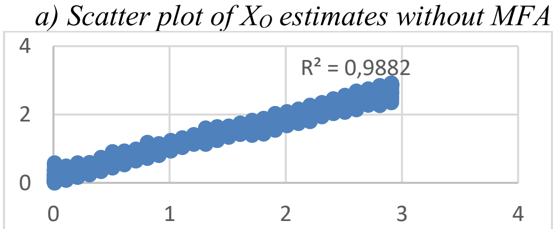

c) Scatter plot of Y_O estimates without MFAT

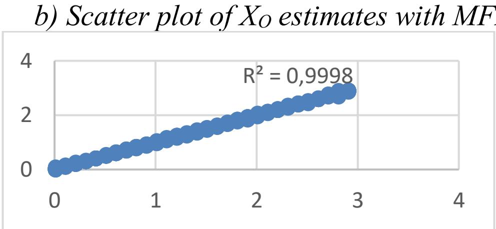

d) Scatter plot of Y_O estimates with MFAT

Figure 3. *Scatter plot of the estimation results in the two cases: MFAT and without MFAT technique.*

The results in Table 1 show that boosting-based models, particularly XGBoost and LightGBM, achieve higher localization accuracy than RF using TOA features. Incorporating the proposed MFAT technique consistently reduces the MAE, RMSE, and MSE of all models by improving TOA estimation quality. Among the evaluated methods, LGBM-MFAT achieved the best performance, with an RMSE of 2.37 cm - approximately 63% lower than the conventional TOA approach and an R^2 of 0.999. This performance is attributed to LightGBM's ability to effectively learn the nonlinear relationship between TOA features and buried-object coordinates, while its histogram-based implementation and leaf-wise tree growth strategy improve computational efficiency for large-scale datasets. Although more sensitive to hyperparameter selection, LightGBM provides an effective trade-off between localization accuracy and computational cost, demonstrating the potential of combining adaptive TOA processing with gradient-boosting models for penetrating IR-UWB localization in heterogeneous environments.

Table 2. *Results of the evaluation metrics.*

	MAE [cm]	RMSE [cm]	R^2	MSE
RF	3.53	6.41	0.993	41.11
RF_MFAT	3.18	4.94	0.997	24.35
XGBoost	2.51	4.66	0.994	21.72
XGBoost _MFAT	2.38	3.29	0.997	10.83
LGBM	1.70	3.01	0.997	9.08
LGBM _MFAT	**1.26**	**2.37**	0.999	5.63

Finally, Table 3 provides a qualitative comparison with representative localization approaches reported in the literature, which were developed using different datasets, propagation environments, radar configurations, sensing modalities, and evaluation protocols. Therefore, the comparison should not be interpreted as a direct quantitative benchmark but rather as a relative performance reference. Conventional GPR image-based localization methods, such as the wide-band chaotic method [20] and multiresolution monogenic signal analysis [21], are often sensitive to propagation conditions, overlapping hyperbolic reflections, and high computational complexity. In contrast, the proposed method was validated using a simulated TOA dataset generated under heterogeneous two-layer environments and evaluated using machine learning models. Under the considered experimental conditions, the proposed LGBM-MFAT method achieved an MAE of 1.26 cm, indicating competitive localization performance. This improvement can be attributed to the MFAT technique, which enhances TOA estimation through matched filtering and adaptive thresholding, thereby improving the quality of the extracted TOA data and enabling the LightGBM model to more effectively learn the nonlinear relationship between TOA features and buried-object locations.

Table 3. *Comparison of the errors of the methods.*

Method	MAE [cm]
Wide-band chaotic [20]	10
Multiresolution monogenic signal analysis method [21]	5.8
Proposed LGBM _MFAT	**1.26**

4. CONCLUSIONS

In this paper, we propose a novel buried object localization method based on machine learning techniques for TOA data in penetrating IR-UWB radar systems. Our analysis demonstrates that by applying the matched filter combined with an adaptive threshold technique during TOA preprocessing and selecting an appropriate machine learning model, the adverse effects caused by noise, clutter, and multipath propagation can be significantly mitigated. As a result, the localization performance is substantially improved in heterogeneous multilayer environments. Furthermore, the proposed approach enables boosting-based models, particularly LightGBM, to effectively learn the nonlinear relationship between TOA characteristics and buried object coordinates. Future work will focus on extending the proposed framework to more complex heterogeneous environments, incorporating measured radar data, and developing real-time three-dimensional localization systems based on advanced deep learning architectures.

REFERENCES

[1]. Groves, P. *"Principles of GNSS, Inertial, and Multisensor Integrated Navigation Systems"*. 2nd ed.; Artech House: Boston, MA, USA, (2013).

[2]. Li, M.-G.; Zhu, H.; You, S.-Z.; Tang, C.-Q. *"UWB-Based Localization System Aided With Inertial Sensor for Underground Coal Mine Applications"*. IEEE Sens. J., vol. 20, pp. 6652–6669, (2020).

[3]. Al-Okby, Mohammed Faeik Ruzaij, et al. *"UWB-based real-time indoor positioning systems: A comprehensive review"*. Applied Sciences, vol. 14, no. 23, 11005, (2024).

[4]. Kia, Ghazaleh, Laura Ruotsalainen, and Jukka Talvitie. *"Toward accurate indoor positioning: An RSS-based fusion of UWB and machine-learning-enhanced WiFi"*. Sensors, vol. 22, no. 9, (2022).

[5]. Ma, Weimin, et al. *"Research on indoor positioning system algorithm based on UWB technology"*. Measurement: Sensors, vol. 33, 101121, (2024).

[6]. Kocur, et al. *"Through-the-wall localization of a moving target by two independent ultra wideband (UWB) radar systems"*. Sensors, vol. 13, no. 9, pp. 11969-11997, (2013).

[7]. Ouadfeul, et al. *"Multiscale analysis of 3D GPR data using the continuous wavelet transform"*. Proceedings of the XIII International Conference on Ground Penetrating Radar, Lecce, Italy, 21–25 June 2010.

[8]. Hart, P.E. *"How the Hough transform was invented"*. IEEE Signal Process. Mag., vol. 26, pp. 18–22, (2009).

[9]. Dumin, O.; Plakhtii, V.; Pryshchenko, O.; Pochanin, G. *"Comparison of ANN and Cross-Correlation Approaches for Ultra Short Pulse Subsurface Survey"*. Proceedings of the 15th International Conference on Advanced Trends in Radioelectronics, Telecommunications and Computer Engineering (TCSET), Lviv-Slavske, Ukraine, pp. 381–386, (2020).

[10]. Huyen, N. T., Ha, D. D., & Hiep, P. T. *"Buried objects detection in heterogeneous environment using UWB systems combined with curve fitting method"*. ICT Express, vol. 6, no. 4, pp. 348-352, (2020).

[11]. Rathnayake, R. M. M. R., et al. *"RSSI and machine learning-based indoor localization systems for smart cities"*. Eng, vol. 4, no. 2, pp. 1468-1494, (2023).

[12]. Díez-González, Javier, et al. *"Time-based UWB localization architectures analysis for UAVs positioning in industry"*. Ad Hoc Networks, vol. 157, 103419, (2024).

[13]. Zhang, Y., Wang, H., Liu, J., et al. *"Deep learning-enhanced UWB localization in complex environments: A survey"*. IEEE Access, vol. 13, pp. 12543–12568, (2025).

[14]. Kim, S., Lee, J., and Park, H. *"Hybrid UWB positioning using machine learning for GNSS-denied environments"*. Sensors, vol. 25, no. 4, Art. no. 1187, (2025).

[15]. Wang, H.; Liu, Q.; Zhou, L. *"Underground target localization method for ground penetrating radar based on deep learning"*. Measurement, vol. 253, Art. no. 117647, (2025).

[16]. Thien, Nguyen Thanh, et al. *"Broadband signal source localization using convolutional neural networks combined with coherent signal subspace methods"*. Journal of Military Science and Technology IITE, pp. 115-122, (2025).

[17]. Saad, Mohamed, et al. *"Development of an IR-UWB radar system for high-resolution through-wall imaging"*. Prog. Electromagn. Res. C, vol. 124, pp. 81-96, (2022).

[18]. X. Chen and S. Kiaei. *"Monocycle shapes for ultra wideband system"*. 2002 IEEE International Symposium on Circuits and Systems. Proceedings (Cat. No. 02CH37353), vol. 1, (2002).

[19]. Gavin, Henri P. *"The Levenberg-Marquardt algorithm for nonlinear least squares curve-fitting problems"*. Department of Civil and Environmental Engineering Duke University, (2019).

[20]. Li, Jingxia and Guo, Tian and Leung, Henry and Xu, Hang and Liu, Li and Wang, Bingjie and Liu, Yang. *"Locating Underground pipe using wideband chaotic ground penetrating radar"*. Sensors, Multidisciplinary Digital Publishing Institute, vol. 19, no. 13, p. 2913, (2019).

[21]. Qiao, Lihong and Qin, Yao and Ren, Xiaozhen and Wang, Qifu. *"Identification of buried objects in GPR using amplitude modulated signals extracted from multiresolution monogenic signal analysis"*. Multidisciplinary Digital Publishing Institute, Sensors, vol. 15, no. 12, pp. 30340–30350, (2015).

TÓM TẮT

Nâng cao độ chính xác định vị vật thể bị chôn vùi trong môi trường không đồng nhất sử dụng IR-UWB dựa trên TOA và học máy

Bài báo đề xuất một phương pháp định vị vật thể bị chôn vùi trong môi trường không đồng nhất sử dụng radar IR-UWB dựa trên tham số thời gian đến (TOA) kết hợp với các kỹ thuật học máy. Một mô hình truyền sóng được xây dựng để tạo bộ dữ liệu TOA cho nhiều vị trí vật thể khác nhau trong điều kiện đa đường và có nhiễu. Để nâng cao độ chính xác của việc ước lượng TOA, kỹ thuật lọc phối hợp kết hợp ngưỡng thích nghi (MFAT) được đề xuất nhằm cải thiện khả năng phát hiện xung phản xạ trong điều kiện SNR thấp. Các đặc trưng TOA thu được sau đó được sử dụng để huấn luyện các mô hình Random Forest (RF), XGBoost và LightGBM (LGBM) cho bài toán định vị vật thể. Kết quả thực nghiệm cho thấy phương pháp LGBM-MFAT đạt hiệu năng tốt nhất với MAE bằng 1,26 cm, RMSE bằng 2,37 cm và hệ số xác định R^2 đạt 0,999. Các kết quả này chứng minh rằng việc kết hợp xử lý TOA thích nghi với các mô hình tăng cường dựa trên cây quyết định giúp cải thiện đáng kể độ chính xác định vị và cung cấp một giải pháp hiệu quả cho các hệ thống radar IR-UWB xuyên thấu hoạt động trong môi trường không đồng nhất.

Từ khoá: Công nghệ IR-UWB; Ra đa xuyên thấu mặt đất; TOA; Random Forest; XGBoost; LGBM.